

1 ***INPP5D* expression is associated with risk for Alzheimer's disease and induced by  
2 plaque-associated microglia**

3 Andy P. Tsai<sup>1#</sup>, Peter Bor-Chian Lin<sup>1#</sup>, Chuanpeng Dong<sup>2#</sup>, Miguel Moutinho<sup>1</sup>, Brad T. Casali<sup>1,3</sup>,

4 Yunlong Liu<sup>2</sup>, Bruce T. Lamb<sup>1,4</sup>, Gary E. Landreth<sup>1,5</sup>, Adrian L. Oblak<sup>1,6\*</sup>, Kwangsik Nho<sup>6\*</sup>

5 <sup>1</sup> Stark Neurosciences Research Institute, IUSM, Indianapolis, IN, USA. tandy@iu.edu (A.P.T);

6 pblin@iu.edu (P.B.L); mmoutinh@iu.edu (M.M); glandret@iu.edu (G.E.L); btlamb@iu.edu

7 (B.T.L); aoblak@iupui.edu (A.L.O)

8 <sup>2</sup> Department of Medical and Molecular Genetics, Center for Computational Biology and

9 Bioinformatics, IUSM, Indianapolis, IN, USA. cpdong@iu.edu (C.D); yunliu@iu.edu (Y.L)

10 <sup>3</sup> Department of Neurosciences, Case Western Reserve University, School of Medicine,

11 Cleveland, OH, USA. btc8@case.edu (B.T.C).

12 <sup>4</sup> Department of Medical and Molecular Genetics, IUSM, Indianapolis, IN, USA. btlamb@iu.edu

13 (B.T.L)

14 <sup>5</sup> Department of Anatomy and Cell Biology, IUSM, Indianapolis, IN, USA. glandret@iu.edu

15 (G.E.L)

16 <sup>6</sup> Department of Radiology & Imaging Sciences, IUSM, Indianapolis, IN, USA.

17 aoblak@iupui.edu (A.L.O); knho@iupui.edu (K.N)

18 **Corresponding Author:** \*For correspondence contact

19 Adrian L. Oblak, Department of Radiology & Imaging Sciences, IUSM, Indianapolis, IN, USA,

20 Methodist GH4101, RADY, Indianapolis, IN, 46202, USA. Phone: +1-317-274-0107; Email:

21 [aoblak@iupui.edu](mailto:aoblak@iupui.edu)

22 Kwangsik Nho, Department of Radiology & Imaging Sciences, IUSM, Indianapolis, IN, USA,

23 Methodist GH4101, RADY, Indianapolis, IN, 46202, USA. Phone: +1-317-963-7503; Email:

24 [knho@iupui.edu](mailto:knho@iupui.edu)

25 \*Corresponding author

26 #Contributed equally

27 **Abstract**

28 **Background**

29       Alzheimer's disease (AD) is a progressive neurodegenerative disorder characterized by  
30 cognitive decline, robust microgliosis, neuroinflammation, and neuronal loss. Genome-wide  
31 association studies recently highlighted a prominent role for microglia in late-onset AD (LOAD).  
32 Specifically, inositol polyphosphate-5-phosphatase (*INPP5D*), also known as SHIP1, is  
33 selectively expressed in brain microglia and has been reported to be associated with LOAD.  
34 Although *INPP5D* is likely a crucial player in AD pathophysiology, its role in disease onset and  
35 progression remains unclear.

36 **Methods**

37       We performed differential gene expression analysis to investigate *INPP5D* expression in  
38 LOAD and its association with plaque density and microglial markers using transcriptomic  
39 (RNA-Seq) data from the Accelerating Medicines Partnership for Alzheimer's Disease (AMP-  
40 AD) cohort. We also performed quantitative real-time PCR, immunoblotting, and  
41 immunofluorescence assays to assess *INPP5D* expression in the 5xFAD amyloid mouse model.

42 **Results**

43       Differential gene expression analysis found that *INPP5D* expression was upregulated in  
44 LOAD and positively correlated with amyloid plaque density. In addition, in 5xFAD mice, *Inpp5d*  
45 expression increased as the disease progressed, and selectively in plaque-associated  
46 microglia. Increased *Inpp5d* expression levels in 5xFAD mice were abolished entirely by  
47 depleting microglia with the colony-stimulating factor receptor-1 antagonist PLX5622.

48 **Conclusions**

49       Our findings show that *INPP5D* expression increases as AD progresses, predominantly  
50 in plaque-associated microglia. Importantly, we provide the first evidence that increased  
51 *INPP5D* expression might be a risk factor in AD, highlighting *INPP5D* as a potential therapeutic

52 target. Moreover, we have shown that the 5xFAD mouse model is appropriate for studying  
53 *INPP5D* in AD.

54

55 **Keywords:** Alzheimer's disease (AD), Microglia, INPP5D, AD risk, Plaque

56

57 **Background**

58 Alzheimer's disease (AD) is the most common cause of dementia, with pathogenesis  
59 arising from perturbed  $\beta$ -amyloid (A $\beta$ ) homeostasis in the brain [1]. The mechanisms underlying  
60 the development of the most common form of AD, late-onset AD (LOAD), are still unknown.  
61 Microglia, the primary immune cells in the brain play a crucial role in AD pathogenesis [2].  
62 Recent large-scale genome-wide association studies (GWAS) reported that many genetic loci  
63 associated with LOAD risk are related to inflammatory pathways, suggesting that microglia are  
64 involved in modulating AD pathogenesis [3, 4]. Among the microglia-related genetic factors in  
65 LOAD, a common variant in *INPP5D* (phosphatidylinositol 3,4,5-trisphosphate 5-phosphatase  
66 1), rs35349669, confers an increase in LOAD risk (OR=1.08) [4, 5]. Conversely, the intronic  
67 *INPP5D* variant rs61068452 is associated with a reduced CSF t-tau/A $\beta$ 1-42 ratio, plays a  
68 protective role in LOAD (p=1.48E-07) [6]. *INPP5D* encodes inositol polyphosphate-5-  
69 phosphatase which participates in regulation of microglial gene expression [7]. Specifically,  
70 *INPP5D* inhibits signal transduction initiated by activation of immune cell surface receptors,  
71 including Triggering receptor expressed on myeloid cells 2 (TREM2), Fc gamma receptor  
72 (Fc $\gamma$ R) and Dectin-1 [8]. The conversion of PI(3,4,5)P3 to PI(3,4)P2 is catalyzed by INPP5D  
73 following its translocation from the cytosol to the cytoplasmic membrane. The loss of  
74 PI(3,4,5)P3 prevents the activation of the immune cell surface receptors [9]. Interestingly,  
75 genetic variants of TREM2, Fc $\gamma$ R, and Dectin-1 are also associated with increased AD risk [10-  
76 12] and are potentially involved in regulating INPP5D activity. Inhibiting INPP5D promotes

77 microglial proliferation, phagocytosis, and increases lysosomal compartment size [13]. Although  
78 INPP5D has been shown to play an important role in microglial function, its role in AD remains  
79 unclear.

80 Here, we report that *INPP5D* is upregulated in LOAD, and elevated *INPP5D* expression  
81 levels are associated with microglial markers and amyloid plaque density. Furthermore, in the  
82 5xFAD mouse model, we found a disease-progression-dependent increase in *INPP5D*  
83 expression in plaque-associated microglia. Our results suggest that *INPP5D* plays a role in  
84 microglia phenotypes in AD and is a potential target for microglia-focused AD therapies.

85 **Methods**

86 **Human participants and RNA-Seq**

87 RNA-Seq data were obtained from the AMP-AD Consortium, including participants of the  
88 Mayo Clinic Brain Bank cohort, the Mount Sinai Medical Center Brain Bank (MSBB) cohort, and  
89 the Religious Orders Study and Memory and Aging Project (ROSMAP) cohort.

90 In the Mayo Clinic RNA-Seq dataset [14], the RNA-Seq-based whole transcriptome data  
91 were generated from human samples of 151 temporal cortices (TCX) (71 cognitively normal  
92 older adult controls (CN) and 80 LOAD) and 151 cerebella (CER) (72 CN and 79 LOAD). LOAD  
93 participants met the neuropathological criteria for AD (Braak score  $\geq 4.0$ ), and cognitively normal  
94 participants had no neurodegenerative diagnosis (Braak score  $\leq 3.0$ ).

95 In the MSBB dataset [15], data were generated from human samples from CN, mild  
96 cognitive impairment (MCI), and LOAD participants' parahippocampal gyrus (PHG) and inferior  
97 frontal gyrus (IFG), superior temporal gyrus (STG) and frontal pole (FP). The clinical dementia  
98 rating scale (CDR) was used to assess dementia and cognitive status [16]. LOAD patients had a  
99 CDR  $\geq 0.5$ , while MCI and CN participants had a CDR of 0.5 and 0, respectively. CN participants  
100 had no significant memory concerns. This study included 108 participants (16 CN, 14 MCI, and

101 78 LOAD) for PHG, 137 participants (21 CN, 18 MCI, and 98 LOAD) for STG, 136 participants  
102 (18 CN, 16 MCI, and 102 LOAD) for IFG, and 153 participants (22 CN, 20 MCI, and 111 LOAD)  
103 for FP.

104 In the ROSMAP dataset [17], RNA-Seq data were generated from the dorsolateral  
105 prefrontal cortices of 241 participants (86 CN and 155 LOAD).

## 106 **Animal models**

107 Wild-type (WT) and 5xFAD mice were maintained on the C57BL/6J background (JAX MMRRC  
108 Stock# 034848) for IHC and qPCR studies. Two-, four-, six-, eight-, and twelve-month-old mice  
109 were used. In the PLX5622 study, we used WT and 5xFAD mice maintained on the mixed  
110 C57BL/6J and SJL background [B6SJL-Tg (APPsweP110, PSEN1<sup>M146L</sup>\*L286V) 6799Vas,  
111 Stock #34840-JAX] (Fig. 3e and 3f). The 5xFAD transgenic mice overexpress five FAD  
112 mutations: the APP (695) transgene contains the Swedish (K670N, M671L), Florida (I716V),  
113 and London (V717I) mutations and the PSEN1 transgene contains the M146L and L286V FAD  
114 mutations. Up to five mice were housed per cage with SaniChip bedding and  
115 LabDiet® 5K52/5K67 (6% fat) feed. The colony room was kept on a 12:12 hr. light/dark  
116 schedule with the lights on from 7:00 am to 7:00 pm daily. They were bred and housed in  
117 specific-pathogen-free conditions. Both male and female mice were used.

## 118 **PLX5622 animal treatment**

119 At four months of age, either normal rodent diet or PLX5622-containing chow was  
120 administered to 5xFAD mice for 28 days. An additional cohort of four-month-old mice was  
121 treated with PLX5622 or control diet for 28 days, then discontinued from PLX5622 feed and fed  
122 a normal rodent diet for an additional 28 days. At six months of age, this cohort of mice was  
123 euthanized. Plexxikon Inc. provided PLX5622 formulated in AIN-7 diet at 1200 mg/kg [18].

## 124 **Statistical analysis**

125 In the human study, differential expression analysis was performed using *limma* software  
126 [19] to investigate the diagnosis group difference of *INPP5D* between CN, MCI, and LOAD. Age,  
127 sex, and *APOE*  $\epsilon 4$  carrier status were used as covariates. To investigate the association  
128 between *INPP5D* expression levels and amyloid plaque density or expression levels of  
129 microglia-specific markers (*AIF1* and *TMEM119*), we used a generalized linear regression  
130 model with *INPP5D* expression levels as a dependent variable and plaque density or microglia-  
131 specific markers along with age, sex, and *APOE*  $\epsilon 4$  carrier status as explanatory variables. The  
132 regression was performed with the "glm" function from the stats package in R (version 3.6.1).

133 In the mouse study, GraphPad Prism (Version 8.4.3) was used to perform the statistical  
134 analyses. Differential expression analysis of both gene and protein levels between WT and  
135 5xFAD mice was performed using unpaired Student's t-test. The statistical comparisons  
136 between mice with and without PLX5622 treatments were performed with one-way ANOVA  
137 followed by Tukey's posthoc test. Graphs represent the mean and standard error of the mean.

138 **RNA extraction and quantitative real-time PCR**

139 Mice were anesthetized with Avertin and perfused with ice-cold phosphate-buffered  
140 saline (PBS). The cortical and hippocampal regions from the hemisphere were micro-dissected  
141 and stored at -80°C. Frozen brain tissue was homogenized in buffer containing 20 mM Tris-HCl  
142 (pH=7.4), 250 mM sucrose, 0.5 mM EGTA, 0.5 mM EDTA, RNase-free water, and stored in an  
143 equal volume of RNA-Bee (Amsbio, CS-104B) at -80°C until RNA extraction. RNA was isolated  
144 by chloroform extraction and purified with the Purelink RNA Mini Kit (Life Technologies  
145 #12183020) with an on-column DNase Purelink Lit (Life Technologies #12183025). 500 ng RNA  
146 was converted to cDNA with the High-Capacity RNA-to-cDNA Kit (Applied Biosystems  
147 #4388950), and qPCR was performed on a StepOne Plus Real-Time PCR system (Life  
148 Technologies). Relative gene expression was determined with the  $2^{-\Delta\Delta CT}$  method and assessed  
149 relative to *Gapdh* (Mm99999915\_g1). *Inpp5d* primer: Taqman Gene Expression Assay (*Inpp5d*:

150 Mm00494987\_m1 from the Life Technologies). Student's *t*-test was performed for qPCR  
151 assays, comparing WT with 5xFAD animals.

152 **Immunofluorescence**

153 Brains were fixed in 4% PFA overnight at 4°C. Following overnight fixation, brains were  
154 cryoprotected in 30% sucrose at 4°C and embedded. Brains were processed on a microtome as  
155 30 µm free-floating sections. For immunostaining, at least three matched brain sections were  
156 used. Free-floating sections were washed and permeabilized in 0.1% Triton in PBS (PBST),  
157 followed by antigen retrieval using 1x Reveal Decloaker (Biocare Medical) at 85°C for 10 mins.  
158 Sections were blocked in 5% normal donkey serum in PBST for 1 hr. at room temperature (RT).  
159 The following primary antibodies were incubated in 5% normal donkey serum in PBST overnight  
160 at 4°C: IBA1 (Novus Biologicals #NB100-1028 in goat, 1:1000); 6E10 (BioLegend #803001 in  
161 mouse, 1:1000; AB\_2564653); and SHIP1/INPP5D (Cell Signaling Technology (CST) #4C8,  
162 1:500, Rabbit mAb provided by CST in collaboration with Dr. Richard W. Cho). Sections were  
163 washed and visualized using respective species-specific AlexaFluor fluorescent antibodies  
164 (diluted 1:1000 in 5% normal donkey serum in PBST for 1 hr. at RT). Sections were  
165 counterstained and mounted onto slides. For X-34 staining (Sigma, #SML1954), sections were  
166 dried at RT, rehydrated in PBST, and stained for ten mins at RT. Sections were then washed  
167 five times in double-distilled water and washed again in PBST for five mins. Images were  
168 acquired on a fluorescent microscope with similar exposure and gains across stains and  
169 animals. Images were merged using ImageJ (NIH).

170 **Immunoblotting**

171 Tissue was extracted and processed as described above, then centrifuged. Protein  
172 concentration was measured with a BCA kit (Thermo Scientific). 50 µg of protein per sample  
173 was boiled in SDS-PAGE protein sample buffer for 10 mins at 95°C, loaded into 4-12% Bis-Tris

174 gels (Life Technologies) and run at 100 V for 90 mins. The following primer antibodies were  
175 used: SHIP1/INPP5D (CST #4C8 1:500, Rabbit mAb) and GAPDH (Santa Cruz #sc-32233).  
176 Each sample was normalized to GAPDH, and the graphs represent the values normalized to the  
177 mean of the WT mice group at each time point.

178 **Results**

179 ***INPP5D* expression levels are increased in LOAD.**

180 *INPP5D* is a member of the inositol polyphosphate-5-phosphatase (INPP5) family and  
181 possesses a set of core domains, including an N-terminal SH2 domain (amino acids 5-101),  
182 Pleckstrin homology-related (PH-R) domain (amino acids 292-401), lipid phosphatase region  
183 (amino acids 401-866) with C2 domain (amino acids 725-863), and C-terminal proline-rich  
184 region (amino acids 920-1148) with two SH3 domains (amino acids 969-974 and 1040-1051)  
185 (**Fig. 1a**). Differential expression analysis was performed using RNA-Seq data from seven brain  
186 regions from the AMP-AD cohort. Expression levels of *INPP5D* were increased in the temporal  
187 cortex (logFC=0.35, p=1.12E-02; **Fig. 1b**), parahippocampal gyrus (logFC=0.54, p=7.17E-03;  
188 **Fig. 1c**), and inferior frontal gyrus (logFC=0.44, p=2.33E-03; **Fig. 1d**) of LOAD patients with age  
189 and sex as covariates (**Table 1**). Interestingly, *INPP5D* expression was also found to be  
190 increased in the inferior frontal gyrus of LOAD patients compared with MCI subjects  
191 (logFC=0.45, p=6.76E-03; **Fig. 1d**). Results were similar when *APOE* ε4 carrier status was used  
192 as an additional covariate. *INPP5D* remained overexpressed in the temporal cortex  
193 (logFC=0.34, p=2.75E-02), parahippocampal gyrus (logFC=0.53, p=1.08E-02), and inferior  
194 frontal gyrus (logFC=0.42, p=4.35E-03) of LOAD patients. However, we did not find any  
195 differences between the diagnosis groups in the cerebellum, frontal pole, superior temporal  
196 gyrus, or dorsolateral prefrontal cortex (**Table 1**). To examine whether *INPP5D* was associated  
197 with microglia, we analyzed the association between *INPP5D* and microglia-specific marker  
198 genes (*AIF1* and *TMEM119*). *AIF1* and *TMEM119* were significantly associated with *INPP5D*

199 expression levels in the parahippocampal gyrus (*AIF1*:  $\beta=0.4386$ ,  $p=4.10E-07$ ; *TMEM119*:  
200  $\beta=0.7647$ ,  $p=<2E-16$ ), inferior frontal gyrus (*AIF1*:  $\beta=0.2862$ ,  $p=6.36E-08$ ; *TMEM119*:  $\beta=0.6109$ ,  
201  $p=<2E-16$ ), frontal pole (*AIF1*:  $\beta=0.2179$ ,  $p=4.53E-04$ ; *TMEM119*  $\beta=0.5062$ ,  $p=4.00E-15$ ), and  
202 superior temporal gyrus (*AIF1*:  $\beta=0.3013$ ,  $p=5.36E-07$ ; *TMEM119*:  $\beta=0.6914$ ,  $p=<2E-16$ ) (**Table**  
203 **2**).

204 ***INPP5D* expression levels are associated with amyloid plaque density in the human**  
205 **brain.**

206 We investigated the association between *INPP5D* expression levels and mean amyloid  
207 plaque densities in four brain regions (**Table 2**). Expression levels of *INPP5D* were associated  
208 with amyloid plaques in the parahippocampal gyrus ( $\beta=0.0212$ ,  $p=3.02E-03$ ; **Fig. 2a**), inferior  
209 frontal gyrus ( $\beta=0.0163$ ,  $p=1.95E-03$ ; **Fig. 2b**), frontal pole ( $\beta=0.0151$ ,  $p=1.22E-02$ ; **Fig. 2c**),  
210 and superior temporal gyrus ( $\beta=0.0220$ ,  $p=5.05E-04$ ; **Fig. 2d**).

211 ***INPP5D* expression levels are increased in an amyloid pathology mouse model**

212 We recapitulated our findings from the human data in the amyloidogenic mouse model,  
213 5xFAD. We observed increased *Inpp5d* mRNA levels in 5xFAD mice throughout disease  
214 progression compared with WT controls in the brain cortex (**Fig. 3a**) and hippocampus (**Fig. 3b**)  
215 of four-, six-, eight-, and twelve-month-old mice (4-months: 1.57-fold in the cortex, 1.40-fold in  
216 the hippocampus; 6-months: 1.86-fold in the cortex, 2.61-fold in the hippocampus; 8-months:  
217 2.23-fold in the cortex and 2.53-fold in the hippocampus; and 12-months: 1.93-fold in the cortex  
218 and 2.16-fold in the hippocampus). Similarly, INPP5D protein levels were increased in the  
219 cortex of 5xFAD mice at four and eight months of age (1.79 and 3.31-fold, respectively;  $p=0.06$ )  
220 (**Fig. 3c and 3d**). To assess *Inpp5d* induction was dependent on microglia, we depleted  
221 microglia in four-month-old 5xFAD mice by treating the animals with the colony-stimulating  
222 factor receptor-1 antagonist PLX5622 (PLX) for 28 days [18]. PLX treatment completely  
223 abolished the increase of *Inpp5d* in 5xFAD mice (**Fig. 3e**). Furthermore, expression levels of

224 *Inpp5d* were restored after switching from the PLX diet to a normal diet for 28 further days (**Fig.**  
225 **3f**).

## 226 **INPP5D expression levels are increased in plaque-associated microglia**

227 Immunohistochemistry of 5xFAD mice brain slices at eight months old revealed that  
228 *Inpp5d* was mainly expressed in plaque-associated microglia (**Fig. 4**). INPP5D- and IBA1  
229 (AIF1)-positive microglia cluster around 6E10-positive or X-34-positive plaques in the cortex  
230 (**Fig. 4a**) and subiculum (**Fig. 4b**). We did not detect any INPP5D expression in WT control mice  
231 (data not shown). Furthermore, analysis of transcriptomic data of sorted microglia from WT  
232 mouse cortex-injected labeled apoptotic neurons [12] revealed a reduction of *Inpp5d* expression  
233 levels in phagocytic microglia compared with non-phagocytic microglia (**Fig. 4c**), which is in  
234 agreement with the report that INPP5D inhibition promotes microglial phagocytosis [13].

## 235 **Discussion**

236 Although genetic variants in *INPP5D* have been associated with LOAD risk [5, 6, 20, 21],  
237 the role of *INPP5D* in AD remains unclear. We identified that *INPP5D* expression levels are  
238 increased in the brain of LOAD patients. Furthermore, expression levels of *INPP5D* positively  
239 correlate with brain amyloid plaque density and *AIF1* and *TMEM119* (microglial marker gene)  
240 expression [22-24]. We observed similar findings in the 5xFAD amyloidogenic model, which  
241 exhibited an increase in gene and protein expression levels of *Inpp5d* with disease progression,  
242 predominately in plaque-associated microglia, suggesting induction of *Inpp5d* in plaque-  
243 proximal microglia. Similarly, a recent study reported that *Inpp5d* is strongly correlated with  
244 amyloid plaque deposition in the APPPS1 mouse model [25, 26]. These findings are consistent  
245 with the observation of microgliosis in both AD and its mouse models.

246 INPP5D inhibition has been associated with microglial activation and increased  
247 phagocytic activity, which is consistent with our transcriptomic data of sorted microglia from

248 murine brains injected with apoptotic neurons [12], showing a decrease in *Inpp5d* expression in  
249 phagocytic microglia compared to non-phagocytic. These findings support the hypothesis that  
250 an increase in *INPP5D* expression in AD is a part of an endogenous homeostatic microglial  
251 response to negatively control their own activity. However, this “brake” might be excessive in  
252 AD, as reflected in our findings that *INPP5D* expression is elevated in LOAD. *INPP5D*  
253 overexpression might result in microglia with deficient phagocytic capacity, resulting in  
254 increased A $\beta$  deposition and neurodegeneration. Thus, the pharmacological targeting of  
255 *INPP5D* might be a novel therapeutic strategy to shift microglia towards a beneficial phenotype  
256 in AD. Future studies in genetic mouse models are necessary to further clarify the role of  
257 *INPP5D* in microglial function and AD progression.

258 **Conclusions**

259 In conclusion, our results demonstrate that *INPP5D* plays a crucial role in AD  
260 pathophysiology and is a potential therapeutic target. *INPP5D* expression is upregulated in  
261 LOAD and positively correlated with amyloid plaque density. *Inpp5d* expression increases in the  
262 microglia of 5xFAD mice as AD progresses, predominately in plaque-associated microglia.  
263 Future studies investigating the effect of *INPP5D* loss-of-function on microglial phenotypes and  
264 AD progression may allow for the development of microglial-targeted AD therapies.

265 **List of abbreviations**

266 AD: Alzheimer's disease, LOAD: late-onset AD, GWAS: genome-wide association  
267 studies, INPP5D: phosphatidylinositol 3,4,5-trisphosphate 5-phosphatase 1, PI(3,4,5)P3:  
268 phosphatidylinositol (3,4,5)-trisphosphate, PI(3,4)P2: phosphatidylinositol (3,4)-bisphosphate,  
269 CSF: cerebrospinal fluid, OR: odds ratio, CI: confidence interval,  $\beta$ :  $\beta$  coefficient, WT: wild-type,  
270 MCI: mild cognitive impairment, APOE  $\epsilon$ 4: apolipoprotein  $\epsilon$ 4 allele, PFA: paraformaldehyde,

271 PCR: polymerase chain reaction, Seq: sequencing, ANOVA: analysis of variance, qPCR:  
272 quantitative real-time PCR, mAb: monoclonal antibody.

273 **Declarations**

274 **Ethics approval and consent to participate**

275 Animals used in the study were housed in the Stark Neurosciences Research Institute  
276 Laboratory Animal Resource Center at Indiana University School of Medicine and all  
277 experimental procedures were approved by the Institutional Animal Care and Use Committee.

278 **Consent for publication**

279 All participants were properly consented for this study.

280 **Availability of data and materials**

281 The datasets analyzed during the current study are available from the corresponding  
282 author on reasonable request.

283 **Competing interests**

284 The authors declare that they have no competing interests.

285 **Funding**

286 This work was supported by NIA grant RF1 AG051495 (B.T.L and G.E.L), NIA grant RF1  
287 AG050597 (G.E.L), NIA grant U54 AG054345 (B.T.L et al.), NIA grant K01 AG054753 (A.L.O),  
288 NIA grant R03 AG063250 (K.N), and NIH grant NLM R01 LM012535 (K.N)

289 **Author contributions**

290 A.P.T, P.B.L, C.D, Y.L, B.T.L, G.E.L, A.L.O, and K.N designed the study. A.P.T, P.B.L,  
291 C.D, M.M, B.T.C, and K.N performed the experiments and analyzed the data. A.P.T, M.M,

292 G.E.L, A.L.O, and K.N wrote the manuscript. All authors discussed the results and commented  
293 on the manuscript.

294 **Acknowledgments**

295 We would like to thank Dr. Richard W. Cho at Cell Signaling Technology for providing  
296 SHIP1/INPP5D Rabbit mAb. We thank Louise Pay for critical comments on the manuscript. We  
297 thank Cynthia M. Ingraham, Deborah D. Baker, Christopher D. Lloyd, Stephanie J. Bissel,  
298 Shweta S. Puntambekar, Guixiang Xu, Roxanne Y. Williams, and Teaya N. Thomas for their  
299 help with taking care of the mice, genotyping, and helpful discussions. We thank the  
300 International Genomics of Alzheimer's Project (IGAP) for providing summary results data for  
301 these analyses. IGAP investigators contributed to the design and implementation of IGAP  
302 and/or provided data but did not participate in analysis or writing of this report. IGAP was made  
303 possible by the generous participation of the control subjects, the patients, and their families.  
304 The i-Select chips were funded by the French National Foundation on Alzheimer's disease and  
305 related disorders. EADI was supported by the LABEX (laboratory of excellence program  
306 investment for the future) DISTALZ grant, Inserm, Institut Pasteur de Lille, Université de Lille 2,  
307 and the Lille University Hospital. GERAD/PERADES was supported by the Medical Research  
308 Council (Grant n° 503480), Alzheimer's Research UK (Grant n° 503176), the Wellcome Trust  
309 (Grant n° 082604/2/07/Z) and German Federal Ministry of Education and Research (BMBF):  
310 Competence Network Dementia (CND) grant n° 01GI0102, 01GI0711, 01GI0420. CHARGE was  
311 partly supported by the NIH/NIA grant R01 AG033193 and the NIA AG081220 and AGES  
312 contract N01-AG-12100, the NHLBI grant R01 HL105756, the Icelandic Heart Association, and  
313 the Erasmus Medical Center and Erasmus University. ADGC was supported by the NIH/NIA  
314 grants: U01 AG032984, U24 AG021886, U01 AG016976, and the Alzheimer's Association grant  
315 ADGC-10-196728.

316

317 **References**

318 1. Lee CY, Landreth GE: **The role of microglia in amyloid clearance from the AD brain.**  
319 *J Neural Transm (Vienna)* 2010, **117**(8):949-960.

320 2. Mandrekar-Colucci S, Landreth GE: **Microglia and inflammation in Alzheimer's**  
321 **disease.** *CNS Neurol Disord Drug Targets* 2010, **9**(2):156-167.

322 3. Karch CM, Goate AM: **Alzheimer's disease risk genes and mechanisms of disease**  
323 **pathogenesis.** *Biol Psychiatry* 2015, **77**(1):43-51.

324 4. Lambert JC, Ibrahim-Verbaas CA, Harold D, Naj AC, Sims R, Bellenguez C, DeStafano  
325 AL, Bis JC, Beecham GW, Grenier-Boley B *et al*: **Meta-analysis of 74,046 individuals**  
326 **identifies 11 new susceptibility loci for Alzheimer's disease.** *Nat Genet* 2013,  
327 **45**(12):1452-1458.

328 5. Jing H, Zhu JX, Wang HF, Zhang W, Zheng ZJ, Kong LL, Tan CC, Wang ZX, Tan L, Tan  
329 L: **INPP5D rs35349669 polymorphism with late-onset Alzheimer's disease: A**  
330 **replication study and meta-analysis.** *Oncotarget* 2016, **7**(43):69225-69230.

331 6. Yao X, Risacher SL, Nho K, Saykin AJ, Wang Z, Shen L, Alzheimer's Disease  
332 **Neuroimaging I: Targeted genetic analysis of cerebral blood flow imaging**  
333 **phenotypes implicates the INPP5D gene.** *Neurobiol Aging* 2019, **81**:213-221.

334 7. Viernes DR, Choi LB, Kerr WG, Chisholm JD: **Discovery and development of small**  
335 **molecule SHIP phosphatase modulators.** *Med Res Rev* 2014, **34**(4):795-824.

336 8. Peng Q, Malhotra S, Torchia JA, Kerr WG, Coggeshall KM, Humphrey MB: **TREM2- and**  
337 **DAP12-dependent activation of PI3K requires DAP10 and is inhibited by SHIP1.** *Sci*  
338 *Signal* 2010, **3**(122):ra38.

339 9. Rohrschneider LR, Fuller JF, Wolf I, Liu Y, Lucas DM: **Structure, function, and biology**  
340 **of SHIP proteins.** *Genes Dev* 2000, **14**(5):505-520.

341 10. Sims R, van der Lee SJ, Naj AC, Bellenguez C, Badarinarayyan N, Jakobsdottir J, Kunkle  
342 BW, Boland A, Raybould R, Bis JC *et al*: **Rare coding variants in PLCG2, ABI3, and**  
343 **TREM2 implicate microglial-mediated innate immunity in Alzheimer's disease.** *Nat*  
344 *Genet* 2017, **49**(9):1373-1384.

345 11. Tsai AP, Dong C, Preuss C, Moutinho M, Lin PB-C, Hajicek N, Sondek J, Bissel SJ,  
346 Oblak AL, Carter GW *et al*: **<em>PLCG2</em> as a Risk Factor for Alzheimer's**  
347 **Disease.** *bioRxiv* 2020:2020.2005.2019.104216.

348 12. Krasemann S, Madore C, Cialic R, Baufeld C, Calcagno N, El Fatimy R, Beckers L,  
349 O'Loughlin E, Xu Y, Fanek Z *et al*: **The TREM2-APOE Pathway Drives the**  
350 **Transcriptional Phenotype of Dysfunctional Microglia in Neurodegenerative**  
351 **Diseases.** *Immunity* 2017, **47**(3):566-581 e569.

352 13. Pedicone C, Fernandes S, Dungan OM, Dormann SM, Viernes DR, Adhikari AA, Choi  
353 LB, De Jong EP, Chisholm JD, Kerr WG: **Pan-SH1P1/2 inhibitors promote microglia**  
354 **effector functions essential for CNS homeostasis.** *J Cell Sci* 2020, **133**(5).

355 14. Allen M, Carrasquillo MM, Funk C, Heavner BD, Zou F, Younkin CS, Burgess JD, Chai  
356 HS, Crook J, Eddy JA *et al*: **Human whole genome genotype and transcriptome data**  
357 **for Alzheimer's and other neurodegenerative diseases.** *Sci Data* 2016, **3**:160089.

358 15. Wang M, Beckmann ND, Roussos P, Wang E, Zhou X, Wang Q, Ming C, Neff R, Ma W,  
359 Fullard JF *et al*: **The Mount Sinai cohort of large-scale genomic, transcriptomic and**  
360 **proteomic data in Alzheimer's disease.** *Sci Data* 2018, **5**:180185.

361 16. Morris JC: **The Clinical Dementia Rating (CDR): current version and scoring rules.**  
362 *Neurology* 1993, **43**(11):2412-2414.

363 17. Bennett DA, Buchman AS, Boyle PA, Barnes LL, Wilson RS, Schneider JA: **Religious**  
364 **Orders Study and Rush Memory and Aging Project.** *J Alzheimers Dis* 2018,  
365 **64**(s1):S161-S189.

366 18. Casali BT, MacPherson KP, Reed-Geaghan EG, Landreth GE: **Microglia depletion**  
367 **rapidly and reversibly alters amyloid pathology by modification of plaque**  
368 **compaction and morphologies.** *Neurobiol Dis* 2020, **142**:104956.

369 19. Ritchie ME, Phipson B, Wu D, Hu Y, Law CW, Shi W, Smyth GK: **limma powers**  
370 **differential expression analyses for RNA-sequencing and microarray studies.**  
371 *Nucleic Acids Res* 2015, **43**(7):e47.

372 20. Farfel JM, Yu L, Buchman AS, Schneider JA, De Jager PL, Bennett DA: **Relation of**  
373 **genomic variants for Alzheimer disease dementia to common neuropathologies.**  
374 *Neurology* 2016, **87**(5):489-496.

375 21. Lambert JC, Heath S, Even G, Campion D, Sleegers K, Hiltunen M, Combarros O,  
376 Zelenika D, Bullido MJ, Tavernier B *et al*: **Genome-wide association study identifies**  
377 **variants at CLU and CR1 associated with Alzheimer's disease.** *Nat Genet* 2009,  
378 **41**(10):1094-1099.

379 22. Hopperton KE, Mohammad D, Trepanier MO, Giuliano V, Bazinet RP: **Markers of**  
380 **microglia in post-mortem brain samples from patients with Alzheimer's disease: a**  
381 **systematic review.** *Mol Psychiatry* 2018, **23**(2):177-198.

382 23. Kaiser T, Feng G: **Tmem119-EGFP and Tmem119-CreERT2 Transgenic Mice for**  
383 **Labeling and Manipulating Microglia.** *eNeuro* 2019, **6**(4).

384 24. Satoh J, Kino Y, Asahina N, Takitani M, Miyoshi J, Ishida T, Saito Y: **TMEM119 marks a**  
385 **subset of microglia in the human brain.** *Neuropathology* 2016, **36**(1):39-49.

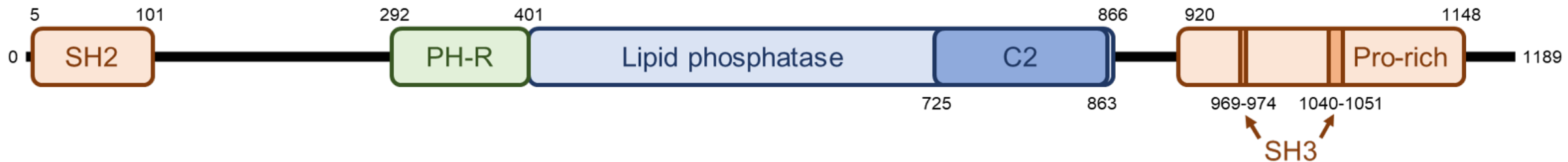
386 25. Radde R, Bolmont T, Kaeser SA, Coomaraswamy J, Lindau D, Stoltze L, Calhoun ME,  
387 Jaggi F, Wolburg H, Gengler S *et al*: **Abeta42-driven cerebral amyloidosis in**  
388 **transgenic mice reveals early and robust pathology.** *EMBO Rep* 2006, **7**(9):940-946.

389 26. Salih DA, Bayram S, Guelfi S, Reynolds RH, Shoai M, Ryten M, Brenton JW, Zhang D,  
390 Matarin M, Botia JA *et al*: **Genetic variability in response to amyloid beta deposition**  
391 **influences Alzheimer's disease risk.** *Brain Commun* 2019, **1**(1):fcz022.



Fig. 1 **Relative quantification of *INPP5D* expression in the studied participants**

a

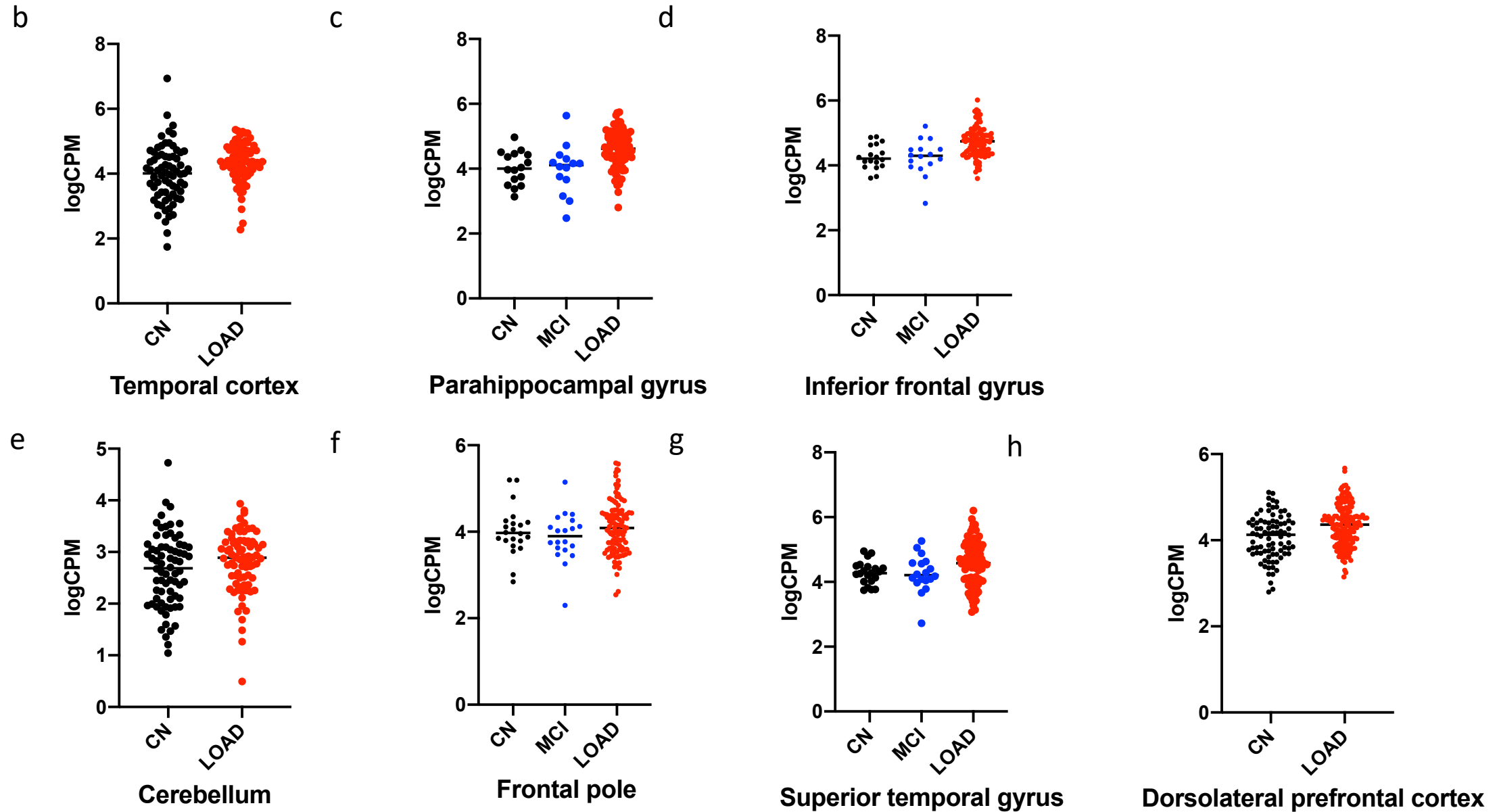


**Fig 1. Relative quantification of *INPP5D* expression in the studied participants**

(a) Domain architecture of *INPP5D* drawn to scale. Gene expression of *INPP5D* is showed as logCPM values in (b) Temporal cortex (TCX)-Mayo, (c) Parahippocampal gyrus (PHG)-MSBB, (d) Inferior frontal gyrus (IFG)-MSBB, (e) Cerebellum (CER)-Mayo, (f) Frontal pole (FP)-MSBB, (g) Superior temporal gyrus (STG)-MSBB, (h) Dorsolateral prefrontal cortex (DLPFC)-ROSMAP.

SH2 *Src Homology 2 domain*, SH3 *SRC Homology 3 domain*, C2 *C2 domain*

Fig. 1

**Relative quantification of *INPP5D* expression in the studied participants**

CN cognitively normal, MCI mild cognitive impairment, LOAD Late-Onset Alzheimer's disease

Table 1.

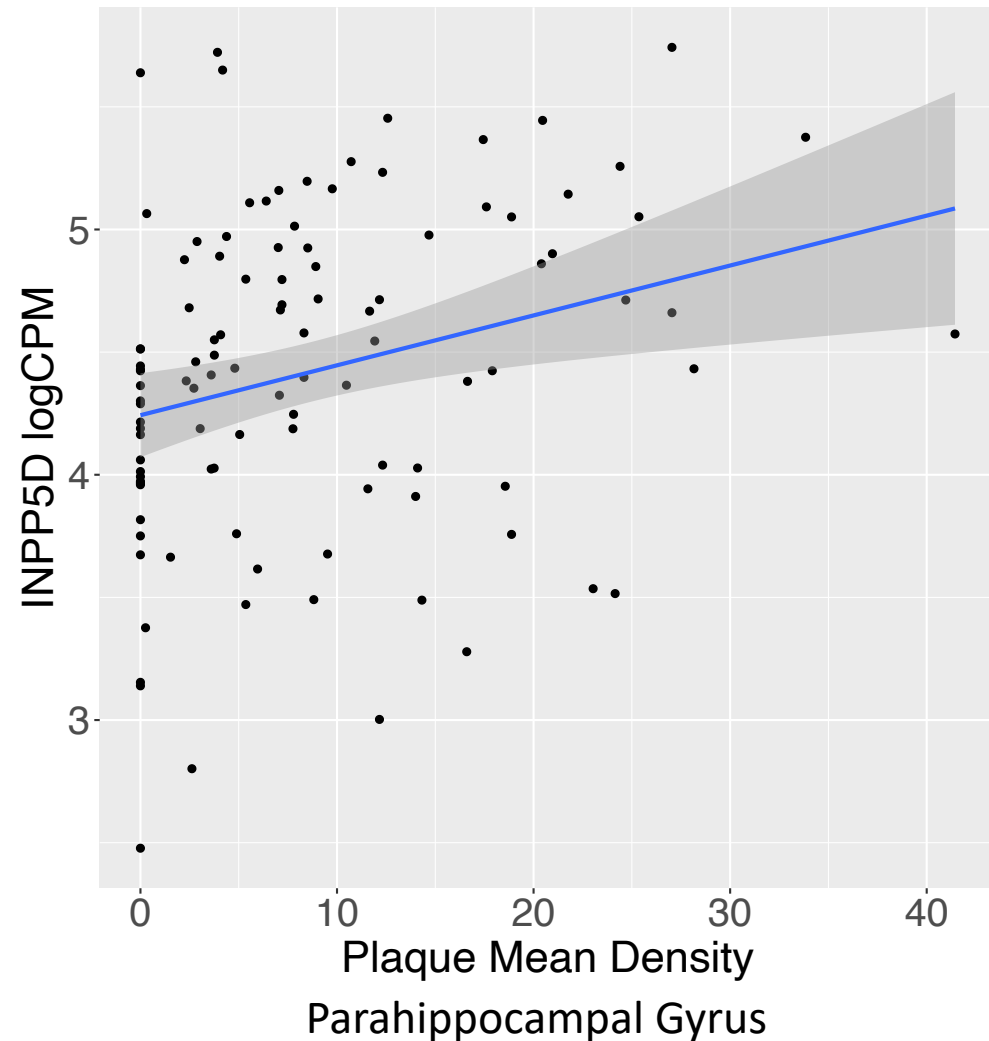
***INPP5D* expression levels were increased in LOAD**

Brain Regions	Temporal Cortex	Parahippocampal Gyrus			Inferior Frontal Gyrus		
Covariate: Age and Sex							
Contrast	CN vs. LOAD	CN vs. MCI	MCI vs. LOAD	CN vs. LOAD	CN vs. MCI	MCI vs. LOAD	CN vs. LOAD
logFC	0.34916854	0.012305567	0.565288103	0.536580956	-0.009944963	0.44545717	0.43695423
p-value	<b>1.12E-02</b>	<b>9.99E-01</b>	<b>7.56E-02</b>	<b>7.17E-03</b>	<b>1.00E+00</b>	<b>6.76E-03</b>	<b>2.33E-03</b>
Covariate: Age, Sex, and APOE ε4 status							
Contrast	CN vs. LOAD	CN vs. MCI	MCI vs. LOAD	CN vs. LOAD	CN vs. MCI	MCI vs. LOAD	CN vs. LOAD
logFC	0.34072691	-0.034336626	0.57213088	0.52809965	-0.0546836	0.46476734	0.42180431
p-value	<b>2.75E-02</b>	<b>1.00E+00</b>	<b>1.00E-01</b>	<b>1.08E-02</b>	<b>1.00E+00</b>	<b>8.00E-03</b>	<b>4.35E-03</b>
Brain Regions	Cerebellum	Frontal Pole			Superior Temporal Gyrus		Dorsolateral Prefrontal Cortex
Covariate: Age and Sex							
Contrast	CN vs. LOAD	CN vs. MCI	MCI vs. LOAD	CN vs. LOAD	CN vs. MCI	MCI vs. LOAD	CN vs. LOAD
logFC	0.15322052	-0.1498388	0.20026554	0.09349678	-0.0115078	0.31887371	0.28945778
p-value	<b>2.15E-01</b>	<b>9.85E-01</b>	<b>4.80E-01</b>	<b>8.65E-01</b>	<b>1.00E+00</b>	<b>2.09E-01</b>	<b>1.78E-01</b>
Covariate: Age, Sex, and APOE ε4 status							
Contrast	CN vs. LOAD	CN vs. MCI	MCI vs. LOAD	CN vs. LOAD	CN vs. MCI	MCI vs. LOAD	CN vs. LOAD
logFC	0.207875239	-0.180168831	0.20013891	0.068420156	-0.020260737	0.282432909	0.22080636
p-value	<b>1.23E-01</b>	<b>9.53E-01</b>	<b>5.13E-01</b>	<b>9.25E-01</b>	<b>1.00E+00</b>	<b>2.89E-01</b>	<b>3.26E-01</b>

Table 1 shows the p-values for the gene expression analyses performed with *limma* using RNA-Seq data from the AMP-AD Consortium. TCX *temporal cortex*, PHG *parahippocampal gyrus*, STG *superior temporal gyrus*, IFG *inferior frontal gyrus*, FP *frontal pole*, CER *cerebellum*, DLPFC *dorsolateral prefrontal cortex*, CN *cognitively normal*, AD *Alzheimer's disease*, MCI *mild cognitive impairment*, logFC *log fold-change*

Fig. 2 **Association of *INPP5D* expression with amyloid plaque mean density**

a



b

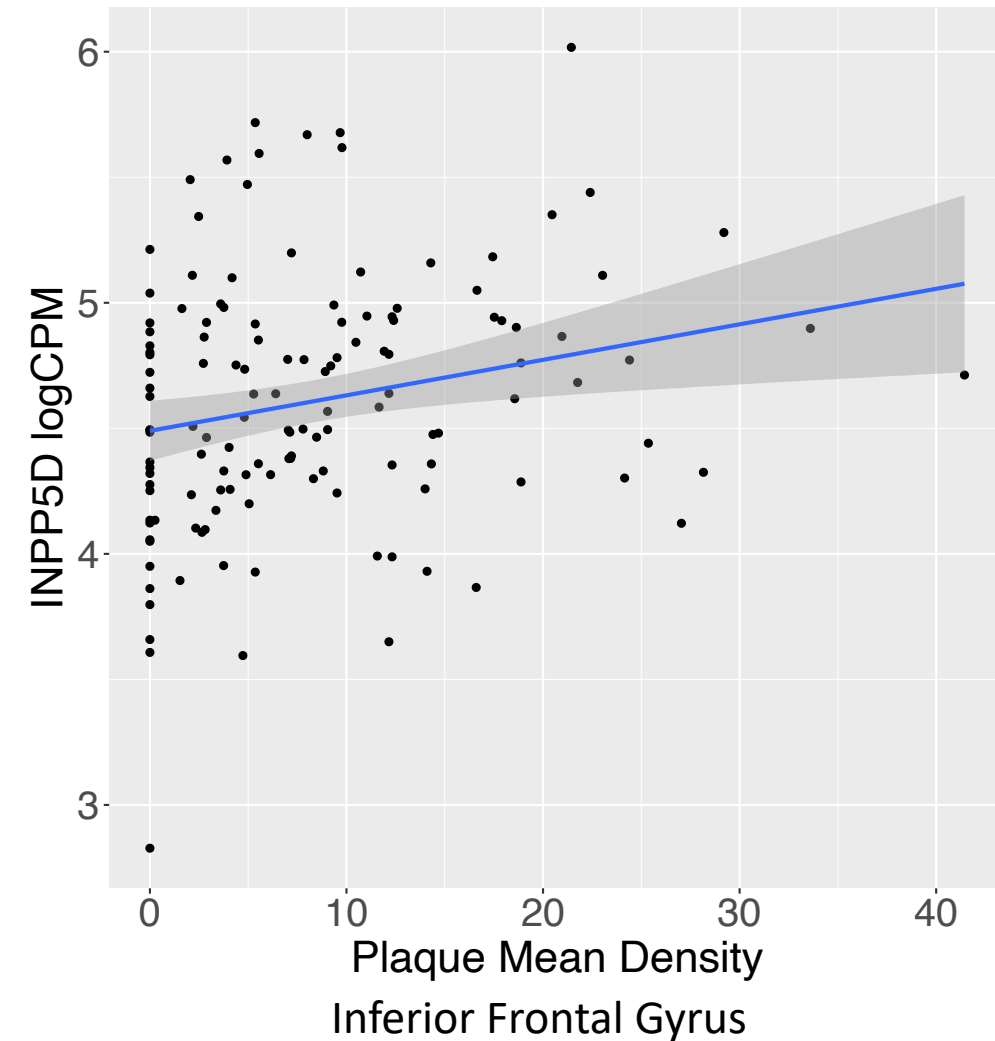
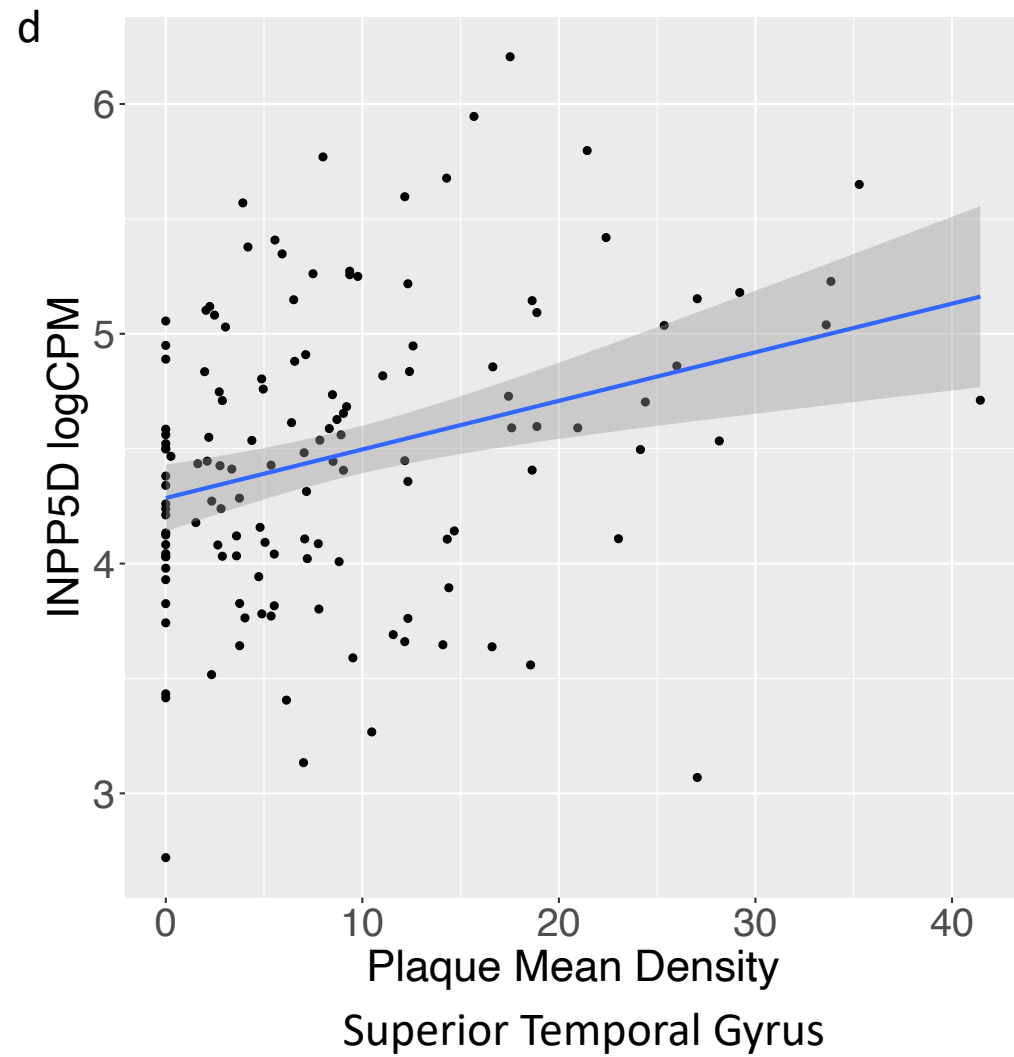
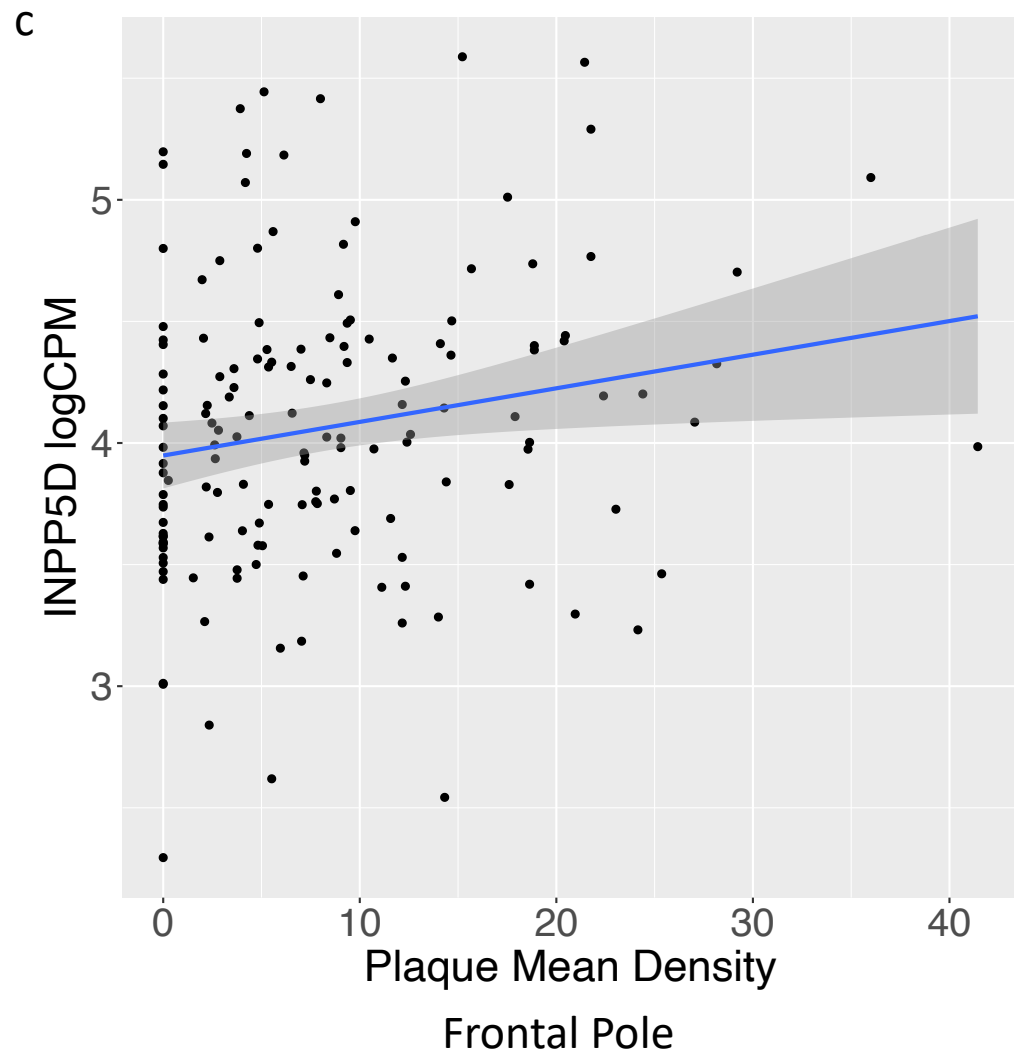


Fig. 2

**Association of *INPP5D* expression with amyloid plaque mean density****Fig 2. Association of *INPP5D* expression with amyloid plaque mean density.**

The scatter plots show the positive association between *INPP5D* expression and plaque mean density in (a) parahippocampal gyrus, (b) inferior frontal gyrus, (c) frontal pole, and (d) superior temporal gyrus from the MSBB cohort.

Table 2.

***INPP5D* expression levels are associated with amyloid plaque density and microglia-specific markers**

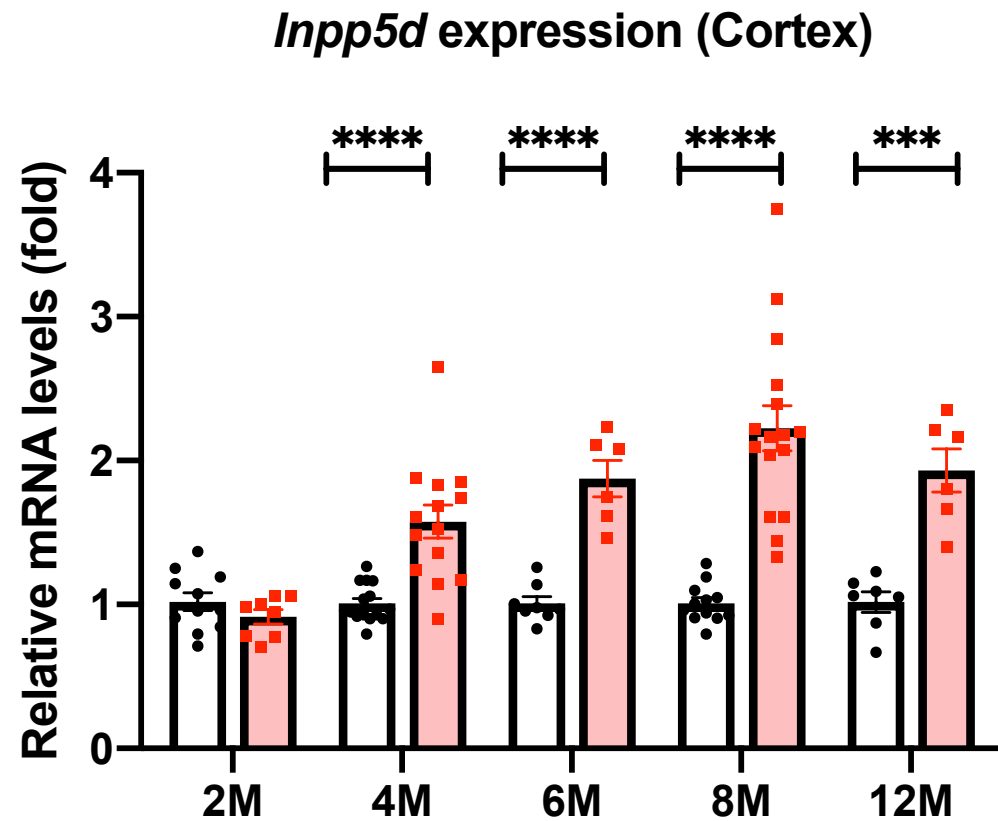
Brain Regions (MSBB)	Parahippocampal Gyrus			Inferior Frontal Gyrus			Frontal Pole			Superior Temporal Gyrus		
	$\beta$	SE	<i>p</i> -value	$\beta$	SE	<i>p</i> -value	$\beta$	SE	<i>p</i> -value	$\beta$	SE	<i>p</i> -value
Plaque Mean Density	0.0212	0.0070	<b>3.02E-03</b>	0.0163	0.0052	<b>1.95E-03</b>	0.0151	0.0059	<b>1.22E-02</b>	0.0220	0.0062	<b>5.06E-04</b>
<i>AIF1</i>	0.4386	0.0811	<b>4.10E-07</b>	0.2862	0.0499	<b>6.36E-08</b>	0.2179	0.0607	<b>4.53E-04</b>	0.3013	0.0572	<b>5.36E-07</b>
<i>TMEM119</i>	0.7647	0.0527	<b>&lt;2E-16</b>	0.6109	0.0446	<b>&lt;2E-16</b>	0.5062	0.0578	<b>4.00E-15</b>	0.6914	0.0496	<b>&lt;2E-16</b>

Table 2 shows the  $\beta$  coefficient ( $\beta$ ), standard error (SE), and *p*-value for the association analysis between *INPP5D* expression levels and amyloid plaque density or expression levels of microglia-specific markers *AIF1* and *TMEM119* by general linear models.

Fig. 3

***Inpp5d* levels are increased in 5xFAD mice**

a



b

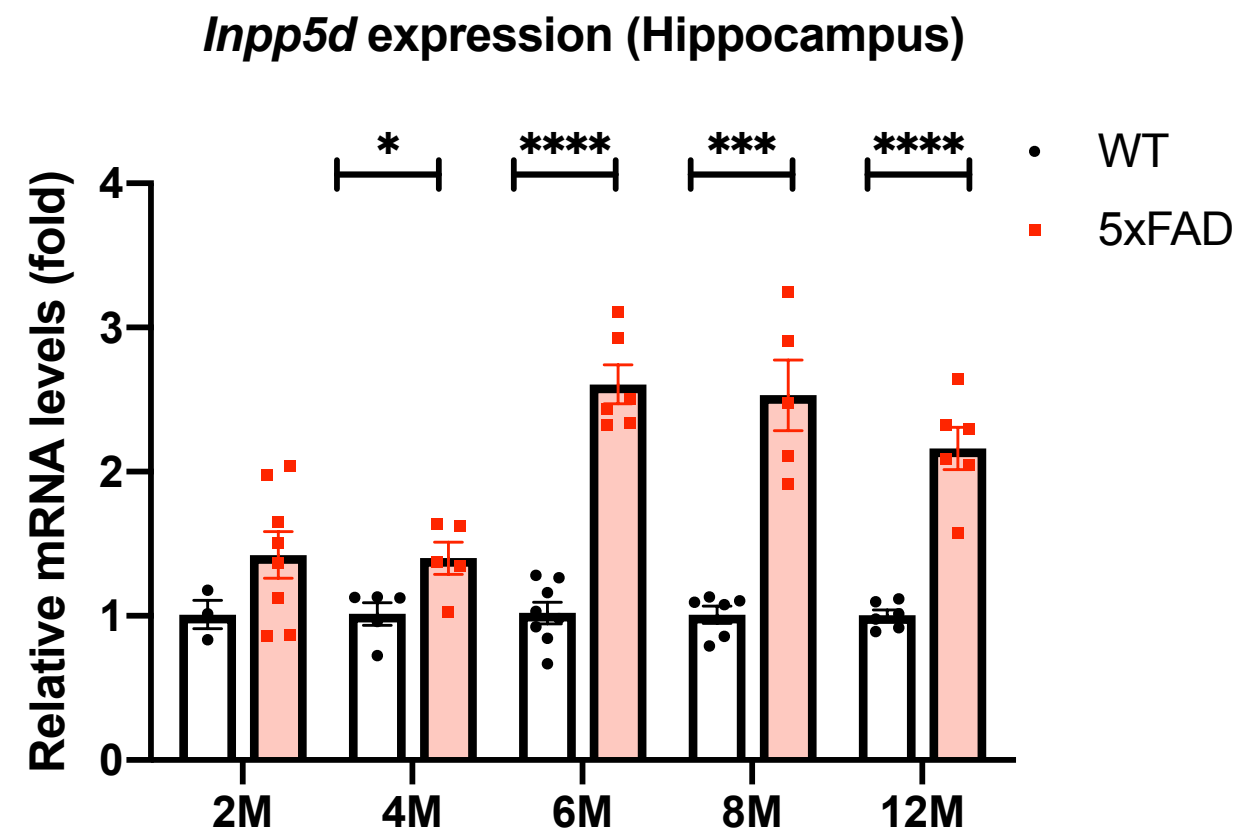
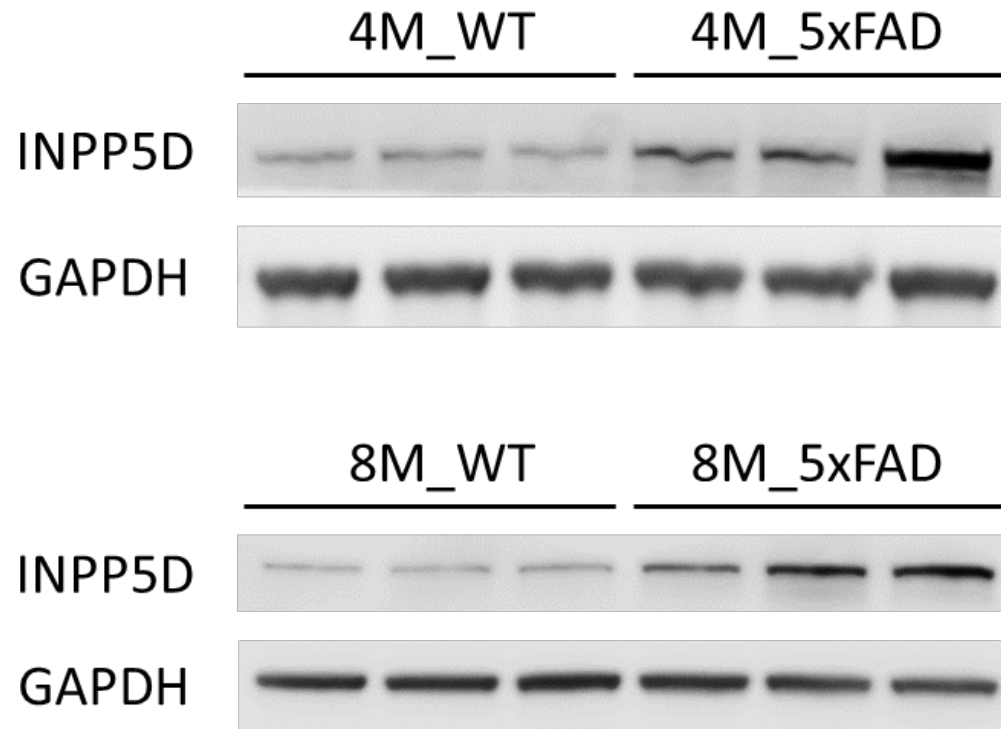


Fig. 3

***Inpp5d* levels are increased in 5xFAD mice**

c



d

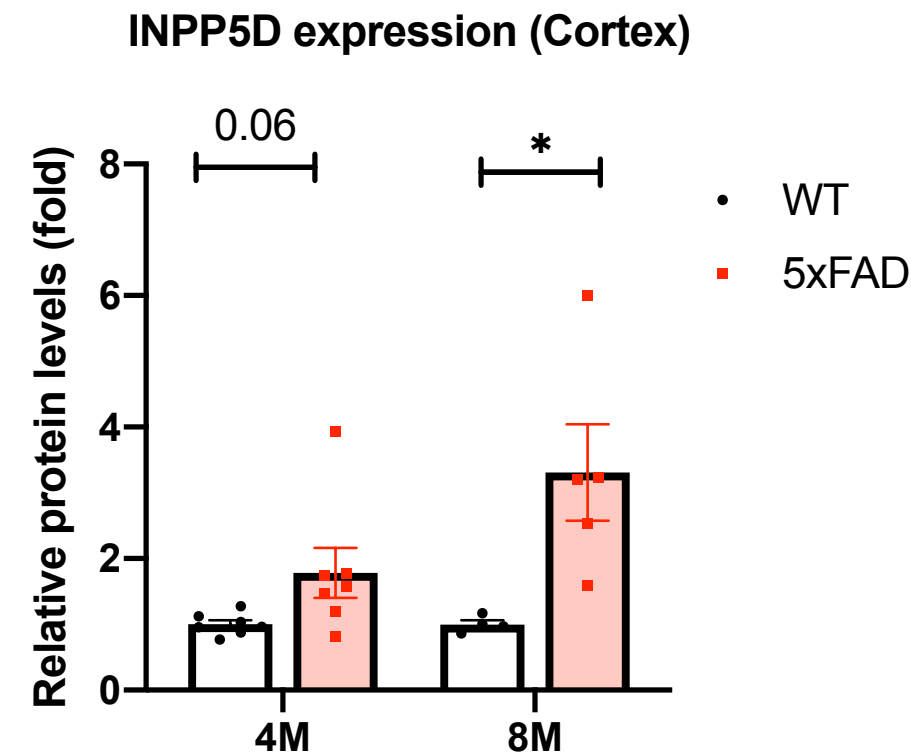
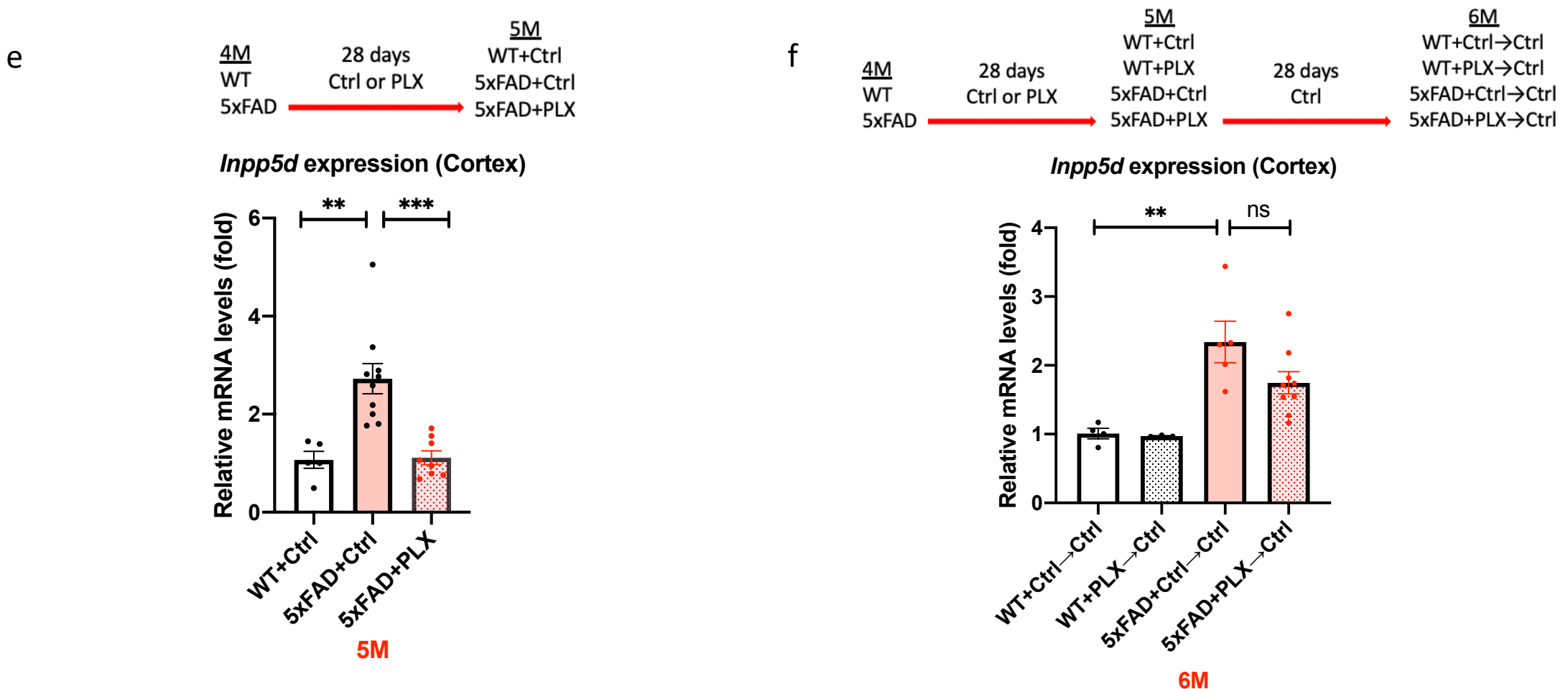


Fig.3

***Inpp5d* levels are increased in 5xFAD mice****Fig 3. *Inpp5d* levels are increased in 5xFAD mice**

Gene and protein levels of *Inpp5d* were assessed in cortical and hippocampal lysates from 5xFAD mice. Gene expression levels of *Inpp5d* were significantly increased in both cortex (a) and hippocampus (b) at 4, 6, 8, and 12 months of age (n=6-15 mice). There were significant changes in *Inpp5d* protein levels in the cortex at 8 months of age and an increased trend in the cortex at 4 months of age (n=4-7). Increased *Inpp5d* levels were abolished with PLX5622 treatment (e), and restored after switching PLX diet to normal diet (f) (n=3-10). \*p<0.05; \*\*p<0.01; \*\*\*p<0.001; \*\*\*\*p<0.0001, ns not significant.

Fig. 4

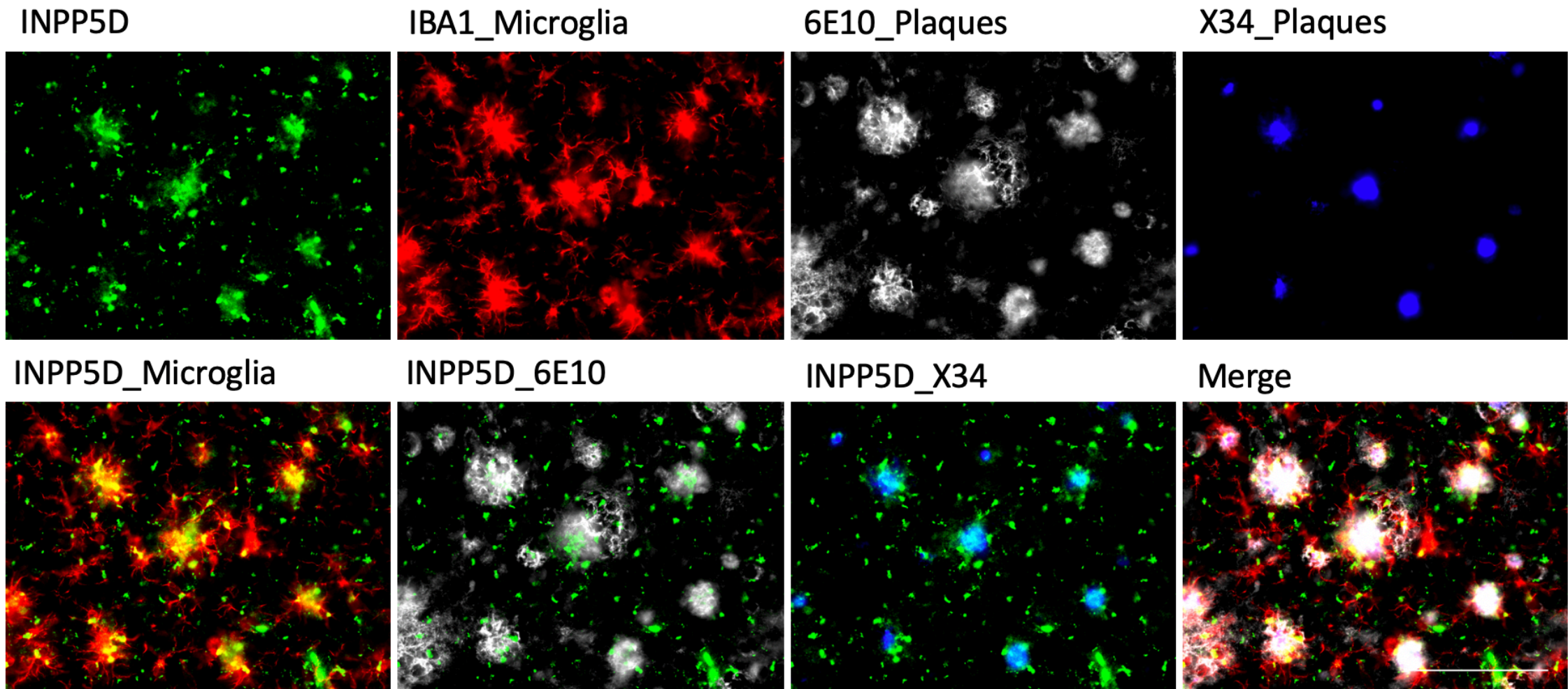
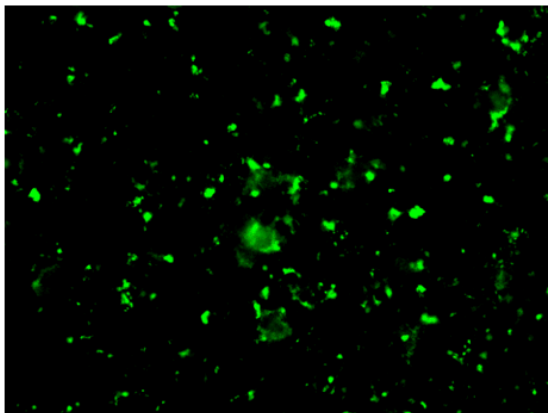
**INPP5D expression levels are increased in plaque-associated microglia.****a Cortex**

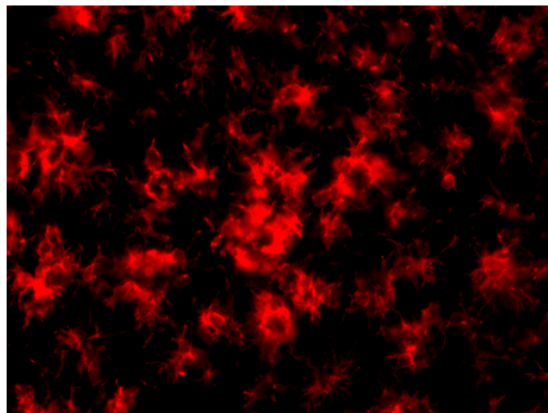
Fig. 4

**INPP5D expression levels are increased in plaque-associated microglia.****b Subiculum**

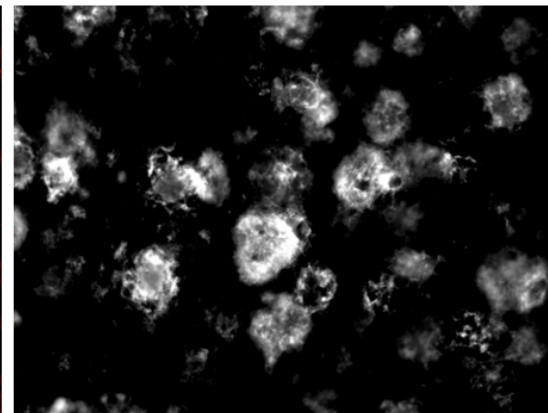
INPP5D



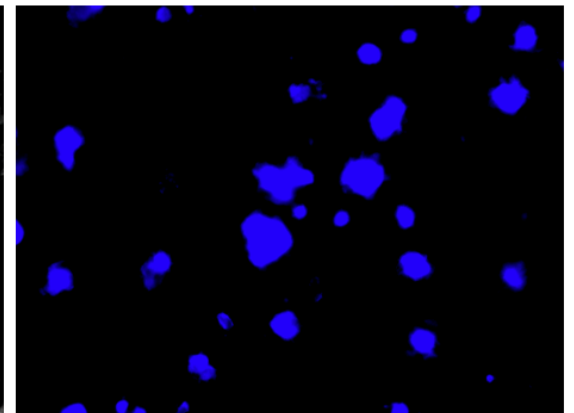
IBA1\_Microglia



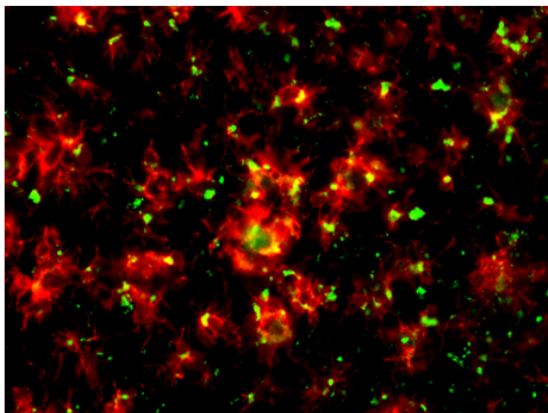
6E10\_Plques



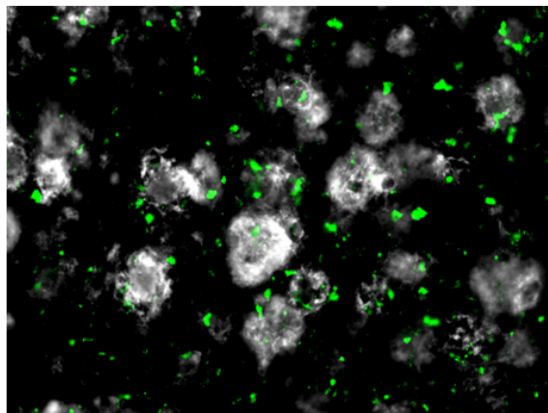
X34\_Plques



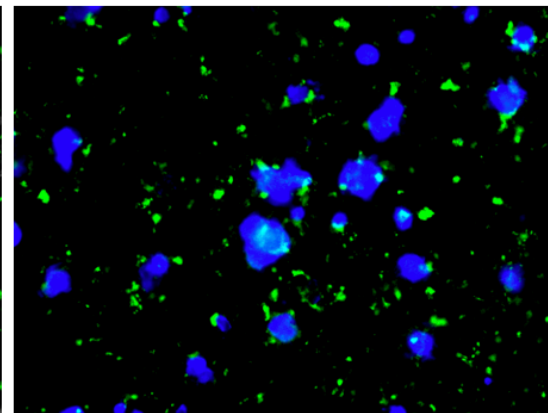
INPP5D\_Microglia



INPP5D\_6E10



INPP5D\_X34



Merge

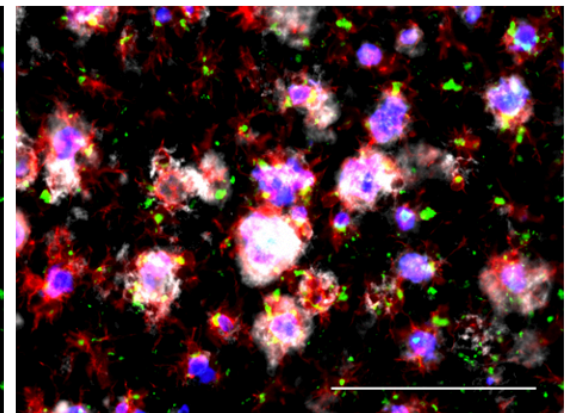
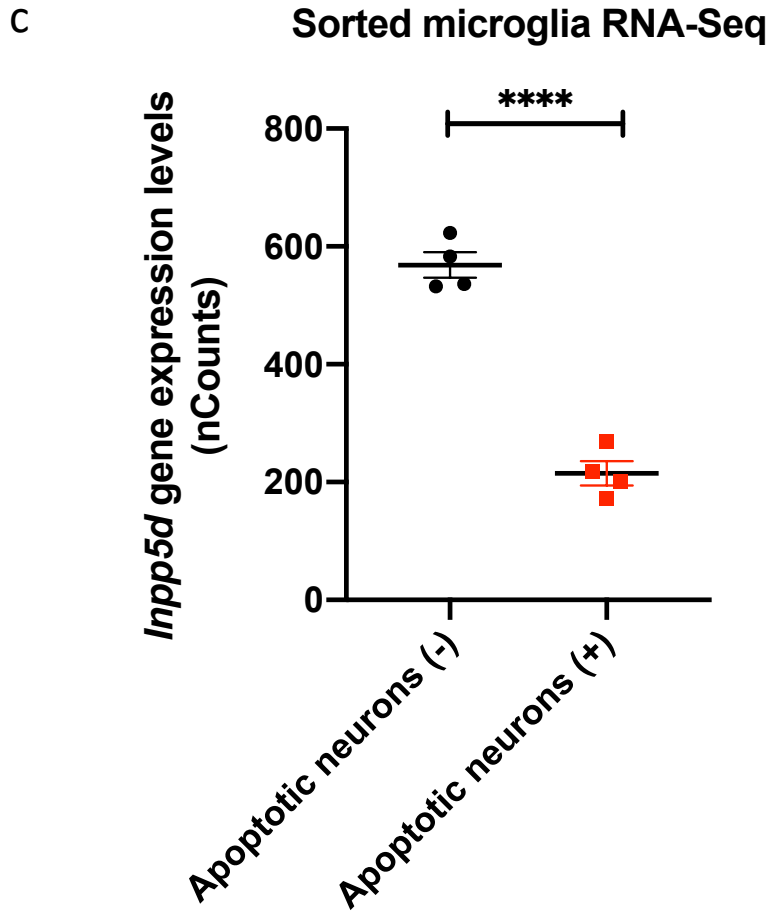


Fig. 4

## INPP5D expression levels are increased in plaque-associated microglia.



**Fig 4. INPP5D expression levels were increased in plaque-associated microglia.** INPP5D was mainly expressed in plaque-associated microglia. INPP5D- and IBA1 (AIF1)-positive microglia cluster around 6E10-positive or X-34-positive plaques in both cortex (a) and subiculum (b) of 8-month-old mice. Analysis of transcriptomic data of sorted microglia from wild-type mice cortex-injected labeled apoptotic neurons revealed that *Inpp5d* expression is increased in non-phagocytic microglia (Krasemann et.al) (c). Scale bar, 10  $\mu$ m. \*\*\*\*p<0.0001